PACS: 79.20.Hx

O.F. Panchenko, L.K. Panchenko

LOW-ENERGY SECONDARY ELECTRON SPECTROSCOPY METHODS IN THE CRYSTAL SUBSURFACE DIAGNOSTICS: APPLICATION TO SOME d-METALS

Donetsk Phys. & Tech. Institute named after A.A. Galkin of the NAS of Ukraine
72, R. Luxembourg St., 83114 Donetsk, Ukraine

Received September 14, 2001

The fine structure (FS) of the experimental secondary electron emission spectra (SEES) along the normal to Ir(111) surface and the target (or total) current spectra (TCS) of Cu(111) surface are interpreted theoretically. It is shown that the FS of SEES and TCS is mainly due to the electronic structure of final states to which the electrons come or from which they emit. The predominant role of the effects of bulk energy-band structure (BES) in the formation of spectra is shown.

Introduction

A detailed study of the near-surface phenomena has become possible owing to a recent development of new investigation techniques and instruments making it possible to determine the composition of a substance and its geometric and electronic structure. The low-energy secondary electron spectroscopy (SES) notable for high surface sensitivity and absence of a destructive action with respect to the investigated sample is among those techniques. The SES, based on the study of phenomena accompanying the process of interaction between the flow of slow-moving primary electrons (PE) I_p (with energy $E_p \leq 1$ keV) and crystal surface, consists of two methods [1,2]: differential and integral ones. The former gives the curve of distribution by the energy of secondary electrons (SE) outside the crystal or SEES. The latter gives the curve of the integrated (or total) current of SE in the sample or TCS.

The main features of the FS of SEES and TCS, showing the whole complex of phenomena taking place in the near-surface layer, are mainly connected with the BES of the crystal [3,4]. SE-emission has been experimentally investigated by many authors; in most cases the objects of investigation were polycrystals. The FS at the background of SEES cascade maximum (CM) was, for example, observed in the energy distribution of SE of the Ir [5], Pt [6], Ag [7,8], Si [9,10], W [3,11-14], Pd [15,16], Ni [17,18], Fe [19,20] and Cu [21-23] single crystals. The theoretical analysis of SEES turned out to be rather difficult because it was necessary to take into consideration all the physical processes taking place at the interaction of PE flow with the crystal. The experimentally observed FS of the SEES could not be explained by the theories within the model of free electrons without taking account of the band structure (BS). Calculations of the SEES done in [3] have shown how the FS relates to the bulk density of states $\rho(E)$; there only the spectral line

position, not shape and intensity, has been analyzed with neglect of the energy level broadening. The FS of SEES has been interpreted in [11,23,24] basing on the theory of low-energy electron diffraction (LEED). The results of [11] differ from those of [3,24] though they satisfactorily describe the FS of the experimental curves. In work [5] the experimental angle-resolved SEES are interpreted as emission from excited bulk bands (some additional features are interpreted as surface resonances) without any theoretical calculations. In so doing, $E(\mathbf{k})$ of the conduction band is calculated by construction of energy E_i of the spectrum peaks as a function of angle emission $\mathbf{k}$. In papers [10,12,25,26] it is shown that the FS of SEES is determined by the energy dispersion of unoccupied high electronic states (located above the vacuum level E_{vac}) and represent the boundaries of bands in the dispersion electrons law (DEL) moving in direction of registering.

A comparatively small number of papers (see, e.g. [2,4,8,27-33]) has been devoted to the investigation of the TCS - the derivative with respect to E_p from total current in circuit of a sample $I = I_p - I_s$, where I_s is the current of electrons, both elastically and nonelastically reflected, emitted from the sample. According to [2,8,27,28], in the energy range to 100 eV the electron-electron (*e-e*) scattering with the excitation of interband transitions prevails, and the main structures in the TCS represent the peculiarities of $\rho(E)$. A relation between the FS of TCS and the BES is also confirmed by calculations done in [31-33] by using the LEED-theory.

The aim of this paper is to elucidate the regularities of SEES and TCS FS formation, their relation with the BES and to develop a technique for the processing of experimental results to obtain the maximum of information on the DEL above E_{vac}. The energy dependence of the band energy level broadening $\hbar\Gamma(E)$, the *e-e-* and electron-plasmon (*e-pl*) contribution to the nonequilibrium SE distribution function $f(E)$, the isotropic component of current from the electrons scattered on the surface were taken into consideration.

Theoretical model

As before, (see, e.g. [10,12,34,35]) during the calculation of the Ir(111) SEES and the Cu(111) TCS the electron scattering with a preset momentum at the crystal was considered within the approximation, when the probability of scattering was proportional to a number of finite states at a given level of E with a preset direction of quasi-momentum $\mathbf{\Omega}$. Here the current through the sample is

$$I(E,\mathbf{\Omega}) = \frac{1}{V}\sum_{n\mathbf{k}} [1 - f_F(E_{n\mathbf{k}})] \left| \frac{1}{\hbar} \nabla_{\mathbf{k}} E_{n\mathbf{k}} \right| \delta(E - E_{n\mathbf{k}})\, \delta(\mathbf{\Omega} - \mathbf{\Omega}_{n\mathbf{k}}), \qquad (1)$$

where $E_{n\mathbf{k}}$ is the DEL; $\mathbf{\Omega}_{n\mathbf{k}}$ is the unit vector along direction $\nabla_{\mathbf{k}} E_{n\mathbf{k}}$; $f_F(E_{n\mathbf{k}})$ is the equilibrium function of occupancy which is zero at $E > E_{vac}$; $E_{vac} = E_F + e\varphi$; E_F is the Fermi level; $e\varphi$ is the work function; V is the volume of the crystal. Passing from summation over $\mathbf{k}$ to integration by the surface of constant energy $E_{n\mathbf{k}} = E$, we obtain (when neglecting the effects of diffraction at crystal surface):

$$I(E,\mathbf{\Omega}) \propto \frac{1}{(2\pi\hbar)^3} \int \frac{\mathrm{d}E'}{\pi} N(E', \mathbf{\Omega}) \frac{\hbar\Gamma(E')/2}{(E - E')^2 + \hbar^2\Gamma^2(E')/4}, \qquad (2)$$

where $N(E,\mathbf{\Omega})$ is the number of energy bands along the direction $\mathbf{\Omega}$, for which the equality $E = E_{n\mathbf{k}}$ is satisfied. The finite width $\hbar\Gamma(E) = \hbar/\tau(E)$ of the electron levels is taken into

account, while the lifetime $\tau(E)$ of the excited state was determined as [36]: $\hbar/\tau(E) \approx$ $\approx E_{pl}(E/E_F - 1)^2$, where E_{pl} is the screening parameter.

The distribution of the electron current with respect to E and $\mathbf{\Omega}$ outside the crystal (disregarding surface diffraction effects) has the form:

$$J(E,\mathbf{\Omega}) \propto \frac{2m(E-E_{vac})\kappa(E)}{(2\pi\hbar)^3}\int \frac{\mathrm{d}E'}{\pi} f(E')N(E',\mathbf{\Omega})\frac{\hbar\Gamma(E')/2}{(E-E')^2+\hbar^2\Gamma^2(E')/4}, \qquad (3)$$

where $\kappa(E) = 4[(E-E_{vac})E]^{1/2}/[(E-E_{vac})^{1/2} + E^{1/2}]^2$ is the transmission coefficient of the crystal-vacuum boundary for one-dimensional motion [37]; $f(E) = f_e(E) + g \times f_{pl}(E)$, where g is the weight. The state occupation function $f_e(E)$, corresponding to multiple *e-e-* scattering, has been obtained in [38] at $E - E_F << E_p$ by solving a system of transport equations within the approximation of *e-e*-scattering statistical model. This system describes the cascade process of the inelastic scattering of the PE flow. Decay of plasmons, generated by the PE as well as by the excited electrons in a solid, contributes to $f(E)$ which, when neglecting the plasmon dispersion, has been obtained in [12] from the energy conservation law:

$$f_{pl}(E) \approx \tau(E)\int_{E_0}^{E_F} \frac{\mathrm{d}E'}{\pi} \frac{\rho(E')\frac{\hbar\Gamma_{pl}}{2}}{(E-E'-\hbar\omega_{pl})^2+\frac{\hbar^2\Gamma_{pl}^2}{4}} \qquad (4)$$

where $\rho(E)$ is the density of filled states; $E_0 = 0$ is the bottom of the valence band; $\hbar\Gamma_{pl}$ is the half-width of the bulk plasmon peak at energy $\hbar\omega_{pl}$ in the spectra of characteristic energy losses of electrons.

Expressions (2) and (3) are valid when $\mathbf{\Omega}$ coincides with the axis of symmetry of a crystal (at normal incidence of the electron beam on the sample). The paper is based on real BS $E_{n\mathbf{k}}$ and $\rho(E)$ [39-41]. $E_{n\mathbf{k}}$ enters the calculation of spectra through the step-like function $N(E,\mathbf{\Omega})$ (see, e.g. fig. 1,*a*). As to the taking into consideration the surface effects which contribute to the formation of $N(E,\mathbf{\Omega})$, the following can be said. The specific features of the electronic spectrum of metal surface are connected with the fact that the electronic spectrum, typical of the bulk, is not practically disturbed in the near-surface region, and the local surface states appear only on its background. This is confirmed by the data of numerous photoemissive investigations [42]. The geometric structure of surface lattices of atomic-pure metal surfaces does not, as a rule, differ from structure of bulk.

Results of the SEES calculation

Fig. 1,*b* shows the results of SEES calculation (according to (3)) along the normal to Ir(111) surface with the attraction of BES obtained by different authors. The background component of current – a structureless CM (peak *A* in fig. 1) was taken into account by the addition of constant C to $N(E,\mathbf{\Omega})$ when the electronic structure (ES) of the near-surface region is described by a model of nearly free electron gas. As is shown in [10], the varying of C in a wide limit from 0 to 100 does not practically change the type of second derivative $J''(E,\mathbf{\Omega})$ which is explained by a small dependence of $J''(E,\mathbf{\Omega})$ on the background component for all E, except for the neighbourhood of CM. For $J(E,\mathbf{\Omega})$ calculation the following values of parameters have been used: $C = 4$ (gives CM shape and width close to

the experiment); $E_F = 10.8$ eV; $e\varphi = 5.8$ eV; $g = 10^{-3}$; $\hbar\Gamma_{pl} = 10.4$ eV at $\hbar\omega_{pl} = 14.8$ eV (according to [43]).

Curve *3* the best agrees with the FS (peaks *B*, *C* and *D*) of experimental spectrum [5] (curve 1), when the parameter of broadening E_{pl}, depending on concentration of *s*- and *d*-electrons in the electronic shell of an atom, was calculated starting not from the general theory of metals (as for curve 2) but was a fitted one. This is because $\tau(E)$, responsible for peak broadening and used in calculations, has been obtained in [36] near the Fermi surface and not in the region of high-lying excited states. Position and intensity of the FS maxima *C* and *D* on curve *4* are essentially different from analogous peculiarities of the experimental spectrum which is because of the approximate calculations of the BS [40] within the RAPW-method for $E \geq 15$ eV above E_F. With the BS calculation [41] within the RKKR-method, to identify the FS of the experimental spectrum (see curve *5*) was not a success.

As is seen from fig. 1, the jumps of the function $N(E,\mathbf{\Omega})$ correspond to extreme values of $J(E,\mathbf{\Omega})$. These jumps or thresholds are formed at boundaries of bands of the resolved energy values for each of the energy bands. Presence of large background component in Ir(111) SEES in the neighbourhood of CM (fig. 1, curve *1*) disables one to distinguish between the bulk and surface effects in the spectrum (a similar situation was observed by us in [26] during the interpretation of Ge(111) SEES). As is shown in [10], the double differentiation of the spectrum could eliminate these difficulties. Apart from this, separation of the bulk and surface properties is also possible when investigating the SEES under the absorption of dissimilar particles [5,6,14,15,44,45]. And the change of FS features serves a measure of the presence of defects in the near-surface layer of the sample, which can be successfully used to control surface states during the processing.

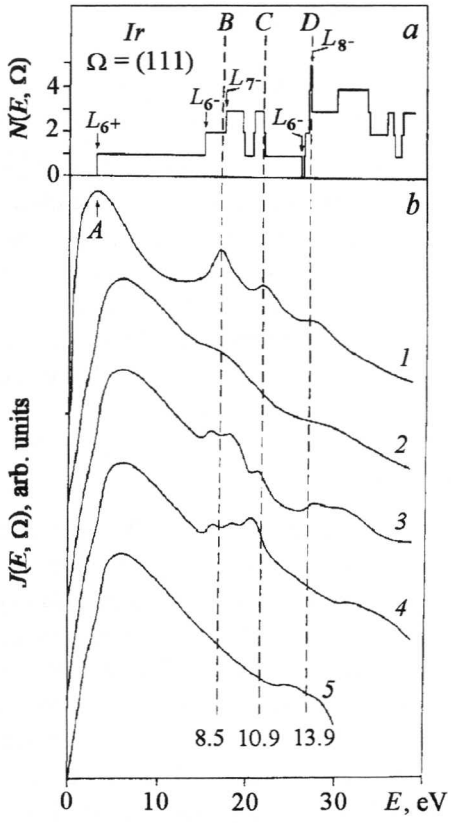

Fig. 1. (*a*) is a number of Ir DEL branches [39] (L_{6+}, L_{6-}, Γ_{6-}, Γ_{7-}, Γ_{8-} its points of symmetry) that intersect the level *E* along the direction **Ω**; (*b*) is the SEES along the normal to (111) surface: *1* – experiment (from paper [5] for the ΓLW azimuth) for $E_p = 40$ eV; *2* – theory based on BS calculations [39] at $E_{pl} = 0.96$ eV; *3–5* – theory based on BS calculations [39], [40] and [41], respectively, at $E_{pl} = 0.27$ eV. Curves *1–5* are plotted on the ordinate arbitrarily. The energy *E* is referred to E_{vac}. Vertical dotted lines with the lettering *A* – *D* show the main singularities of the experimental SEES.

Results of the TCS calculation

The results of the TCS $S(E,\Omega)$ calculation (according to (2)) are shown in fig. 2 (curves *3,4*) for Cu(111). In calculations the following values of parameters have been used: $E_F = 9.2$ eV; $e\varphi = 4.2$ eV; $E_{pl} = 4$ eV. In fig. 2 (curves *1,2* and *5*) the experimental TCS [2,29,31] are shown for comparison. The spectra have FS which is essentially dependent on single-crystal orientation. The intensity of FS ~ 1 % of the value of PE distribution maximum (in figures it is absent), which occurs at the energy when the electrons start hitting the sample. The main peculiarities of the Cu(111) TCS (the maxima *c-g*) are in agreement with the representations on the BES in the near-surface region. On the background of spectrum structure corresponding to the bulk (discussed in [34]), the maxima *a*, *b* (curve *1*) and *b′* (curve *5*) are observed, the formation of which is connected with the excitation of electrons from the occupied states located near E_F. These states are the surface ones, they develop only in the experiments [2], [29] and are not registered in the experiment [31], and are absent on the theoretical curves, constructed without considering both elastic scattering and the surface structure and states. Differences in the position of singularities on theoretical and experimental curves are connected (as was stated above) on one hand, with the approximate character of BS calculation for high-lying levels [40] (according to [32], empty high-positioned electron states, contrary to the universally accepted point of view, can be characterized by considerable deviations from the free electron dispersion, and influenced by multi-electron effects). On the other hand, there exist the experimental errors connected with the formation of collimated electron beam in the region of low energies, realization of the total collection of SE, etc. Thus, the energy position and the intensity of maxima in the TCS of Cu(111) highly depend on the angle of primary beam incidence [27]. Singularity *d* (curve *1*) abruptly decreases when the electron beam deviates from the normal to the surface. In the experiment this fact was used as a criterion of conditions for the normal incidence of primary beam. Singularities *a*, *b* and *b′* can be explained by both the high surface sensitivity of the TCS determined not only by a small depth of the analysed region, but by a high dependence on the physical and chemical surface processes [28,30], and the deviation of the electron beam from the normal, with some error in the orientation of faces. Note that the absorption of residual gases (~ 10^{-2} Pa) on Cu(111) surface or the ionic bombardment thereof also results in maxima *a* and *b* vanishing; subsequent desorption of residual gases is accompanied

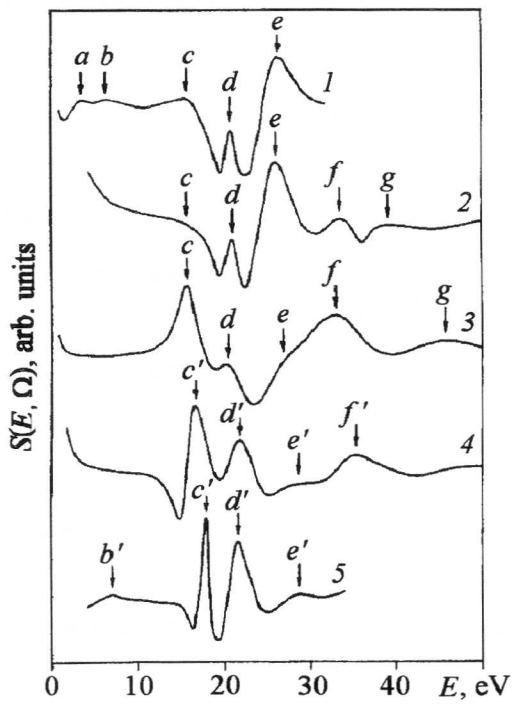

Fig. 2. TCS along the normal to Cu(111) surface: *1*, *2* – the experimental results $dI(E,\Omega)/dE$ from [2] and [31], respectively; *3* – theory $dI(E,\Omega)/dE$; *4* – theory $d^2I(E,\Omega)/dE^2$; *5* – experiment $d^2I(E,\Omega)/dE^2$ from [29]. Curves *1–5* are plotted on the ordinate arbitrarily. The energy E is referred to E_{vac}. The positions of TCS typical maxima are denoted by *a,b,c,...,f′* in energy increasing.

by the restoration of their intensity [2]. The absorbents or dissimilar atoms and defects present on the surface result in the large-angle elastic scattering, thus opening new channels for the electron penetration to the crystal.

Conclusion

The obtained correspondence between the main features of experimental and theoretical SEES and TCS of some d-metals evidences the prevailing role of the BES effects in the formation of spectra. And there occurs a possibility for the experimental study of DEL in the region of energies much higher than Evac and for usage of the SEES and TCS data in a more perfect calculation of BS showing which singularities of the spectra relate to some or other bands. Investigation and interpretation of the experimental SEES and TCS at different angles of PE incidence can give a straightforward information on the BES features in the whole of the Brillouin zone. It can be used for the analysis of the photoemission and inverse photoemission spectroscopy data. The dependence of SEES and TCS FS on geometrical structure and degree of ordering of the investigated crystals has been confirmed. Alongside with singularities responding to BES, the singularities connected with the electron transitions with the participation of surface states develop in the spectra (see fig. 2 for TCS and [5] for SEES of the clean Ir(111) surface (ΓLK azimuth) and with (2x1)O overlayer). The method being developed enables one to distinguish between the bulk effects in SEES and TCS and the surface ones which are to be investigated separately [46] (this can be successfully used for the control of surface states during processing).

This study was supported by the Government Fund for Basic Research of Ukraine.

1. *A.R. Shul'man, and S.A. Fridrikhov*, Secondary Emission Methods in Solid State Research, Nauka, Moscow (1977) (in Russian).
2. *S.A. Komolov*, Total Current Spectroscopy of Surface, Gordon & Breach, Philadelphia (1992).
3. *N.E. Christensen, and R.F. Willis*, J. Phys. C: Sol. State Phys. **12**, 167 (1979).
4. *I. Schäfer, M. Schlüter, and M. Skibowski*, Phys. Rev. **B35**, 7663 (1987).
5. *J.U. Mack, E. Bertel, F.P. Netzer, and D.R. Lloyd*, Z. Phys. B: Condens. Matter **63**, 97 (1986).
6. *B. Lang*, Surf. Sci. **66**, 527 (1977).
7. *M.P. Seah*, Surf. Sci. **17**, 132 (1969).
8. *V.A. Novolodsky, O.M. Artamonov, and S.A. Komolov*, Techn. Phys. **44**, 99 (1999).
9. *P.E. Best*, Phys.Rev. **B19**, 2246 (1979).
10. *V.M. Shatalov, O.F. Panchenko, O.M. Artamonov, A.G. Vinogradov, and A.N. Terekhov*, Sol. State Comm. **68**, 719 (1988).
11. J. *Schäfer, R. Schoppe, J. Hölzl, and R. Feder*, Surf. Sci. **107**, 290 (1981).
12. *V.V. Korablev, Yu.A. Kudinov, O.F. Panchenko, L.K. Panchenko, and V.M. Shatalov*, Phys. Solid St. **36**, 1290 (1994).
13. *L.N. Tharp, and E.J. Scheibner*, J. Appl. Phys. **38**, 3320 (1967).
14. *O.M. Artamonov, and A.N. Terekhov*, Sov. Phys. Solid St. **28**, 479 (1986).
15. *B. Lang, and S. Tatarenko*, Sol. State Comm. **31**, 303 (1979).
16. *D.R. Lloyd, and F.P. Netzer*, Sol. State Comm. **45**, 1047 (1983).
17. *J. Schäfer, and J. Hölzl*, Thin Solid Films **13**, 81 (1972).
18. *H. Hopster, R. Raue, E. Kisker, G. Güntherodt, and M. Campagna*, Phys. Rev. Lett. **50**, 70 (1983).
19. *T. Koshikawa, R. Shimizu, K. Goto, and K. Ishikawa*, J. Phys. D: Appl. Phys. **7**, 462 (1974).
20. *E. Kisker, W. Gudat, and K. Schröder*, Sol. State Comm. **44**, 591 (1982).

21. *G. Appelt*, Phys. Stat. Sol. **27**, 657 (1968).
22. *L.H. Jenkins, and M.F. Chung*, Surf. Sci. **26**, 151 (1971).
23. *K.K. Kleinherbers, A. Goldmann, E. Tamura, and R. Feder*, Sol. State Comm. **49**, 735 (1984).
24. *R. Feder, and J.B. Pendry*, Sol. State Comm. **26**, 519 (1978).
25. *O.F. Panchenko, and L.K. Panchenko*, Sol.State Comm. **89**, 849 (1994).
26. *O.F. Panchenko, and L.K. Panchenko*, Sol.State Comm. **101**, 483 (1997).
27. *S.A. Komolov, and L.T. Chadderton*, Surf. Sci. **90**, 359 (1979).
28. *S. Komolov, E. Lazneva, and P.J. Møller*, Surf. Sci. **323**, 102 (1995).
29. *R.C. Jaklevic, and L.C. Davis*, Phys. Rev. **B26**, 5391 (1982).
30. *A. Dittmar-Wituski, and P.J. Møller*, Surf. Sci. **287/288**, 577 (1993).
31. *Å. Lindgren, L. Walldén, J. Rundgren, and P. Westrin*, Phys.Rev. **B29**, 576 (1984).
32. *V.N.Strocov*. In: *Electron Spectroscopies Applied to Low-Dimensional Materials* /Edited by H.I. Starnberg, H.P. Hughes/, Netherlands, Kluwer (2000).
33. *E. Tamura, R. Feder, J. Krewer, R.E. Kirby, E. Kisker, E.L. Garwin, and F.K. King*, Sol. State Comm. **55,** 543 (1985).
34. *S.A. Komolov, O.F. Panchenko, and L.K. Panchenko*, Phys. Solid St. **38**, 1733 (1996).
35. *O.F. Panchenko, and L.K. Panchenko*, Phys. Lett. **A192**, 289 (1994).
36. *D. Pines, P. Nozières*, The Theory of Quantum Liquids. 1: Normal Fermi Liquids, Benjamin, New York-Amsterdam (1966).
37. *L.D. Landau, and E.M. Lifshitz*, Quantum Mechanics: Non-Relativistic Theory /3rd ed./, Pergamon Press, New York-Oxford (1977).
38. *O.F. Panchenko, and L.K. Panchenko*, J. Electr. Spectr. Rel. Phenom. **83**, 21 (1997).
39. J. *Noffke, and L. Fritsche*, J. Phys. F: Met. Phys. **12**, 921 (1982).
40. *V.V. Nemoshkalenko, V.N. Antonov*, Computational Physics Methods in Solid State Theory. Band Theory of Metals, Naukova Dumka, Kiev (1985) (in Russian).
41. *P.N. Ray, J. Chowdhuri, and S. Chatterjee*, J. Phys. F: Met .Phys. **13**, 2569 (1983).
42. *K.C. Prince*, Photoelectron Spectroscopy of Solids and Surfaces, in: Synchrotron Radiation Techniques and Applications, World Sci.Publ., London (1999).
43. *F.P. Netzer, J.U. Mack, E.Bertel, and J.A.D. Matthew*, Surf. Sci. **160**, L509 (1985).
44. *J.A. Schäfer*, Surf. Sci. **148**, 581 (1984).
45. *W.S. Vogan, S.G. Walton, and R.L. Champion*, Surf. Sci. **459**, 14 (2000).
46. *O.F. Panchenko*, Surf. Sci. **482-5**, 723 (2001).